PHYSICAL REVIEW B **71**, 020502(R) (2005)

Direct determination of localized impurity levels located in the blocking layers of $Bi_2Sr_2CaCu_2O_y$ using scanning tunneling microscopy/spectroscopy

G. Kinoda*
Kanagawa Academy of Science and Technology, 3-2-1 Sakado, Takatsu-ku, Kawasaki, Kanagawa 213-0012, Japan

H. Mashima
Frontier Collaborative Research Center, Tokyo Institute of Technology, 4259 Nagatsutacho, Midori-ku, Yokohama 226-8503, Japan

K. Shimizu, J. Shimoyama, and K. Kishio
Department of Superconductivity, University of Tokyo, 7-3-1 Hongo, Bunkyo-ku, Tokyo 113-8656, Japan

T. Hasegawa†
Department of Chemistry, University of Tokyo, 7-3-1 Hongo, Bunkyo-ku, Tokyo 113-8656, Japan
(Received 19 October 2004; published 7 January 2005)

Local electronic states of the high-T_c superconductor $Bi_{2-x}Pb_xSr_2CaCu_2O_y$ single crystals with $x=0.6$ have been studied using low-temperature scanning tunneling microscopy/spectroscopy (STM/STS). We found that they are modified by substitutional impurities occupying the Sr (or Ca) and Bi site. Individual impurities could be imaged selectively by STM; the Sr(Ca)-site impurities could be seen only for a positive sample bias, whereas the Pb atoms substituting for the Bi sites could be imaged with larger corrugations for a negative bias. STS measurements revealed that the former behaves as a donorlike dopant with an energy of +1.7 eV, consistent with a chemical view indicating that excess Bi^{3+} ions are substituted in the Sr^{2+} sites. On the other hand, the latter gives rise to an acceptorlike state at −1.4 eV near the band edge, which is thought to promote hole doping into the CuO_2 layer.

DOI: 10.1103/PhysRevB.71.020502 PACS number(s): 74.72.Hs, 07.79.Cz, 74.25.Jb, 71.55.−i

In conducting and semiconducting materials, it is crucial to understand the local electronic nature of individual impurity atoms because they not only scatter conducting electrons but also control the amount of mobile carriers. Scanning tunneling microscopy/spectroscopy (STM/STS) is widely recognized as a powerful experimental tool for investigating surface atomic and electronic structures on a nanometer scale. With excellent spatial resolution, this technique has been extensively used to determine electronic properties of individual impurities including ionization energies, Bohr radii, and quantitative charge states in semiconductors.[1–5]

Recently, we reported the results of STM/STS observations of heavily Pb-doped $Bi_{2-x}Pb_xSr_2CaCu_2O_y$ (Pb-Bi2212) superconductors.[6] Pb atoms doped into the surface BiO layer were distinguishable as bright spots with larger corrugations than those of Bi atoms. We also found different types of nanoscale structures attributable to natural impurities occupying Sr or Ca sites. These are unique STM observations of substitutional impurities located in the blocking layers of high-T_c cuprates. However, detailed electronic properties of the substitutional impurities have not been examined yet.

Here, we report STM/STS measurements of heavily Pb-doped Bi2212 single crystals, focusing on local electronic structures around the impurities. Bias-dependent STM results confirmed that Pb atoms and Sr(Ca)-site impurities could be imaged selectively by setting the bias voltage appropriately. Based on the STS spectra obtained, which is a measure of local density of states (LDOS), we discuss the effects of these impurities on the superconductivity, and their electronic roles in the band structure of Bi2212.

$Bi_{2-x}Pb_xSr_2CaCu_2O_y$ single crystals with $x=0.6$ were grown using the floating zone technique. Details of the crystal-growth procedure have been described elsewhere.[7] For the STM/STS observations in this study, we used as-grown crystals without further annealing. The superconducting transition temperature T_c was determined to be ~80 K, using a superconducting quantum interference device (SQUID) susceptometer.

STM/STS measurements were carried out with a home-built ultra-high-vacuum low-temperature STM instrument equipped with a low-temperature cleavage stage.[8] The base pressure of the STM chamber was maintained at less than 2.0×10^{-10} Torr during the measurements. All the Pb-Bi2212 samples examined here were cleaved *in situ* at 77 K, and then immediately transferred to the already refrigerated STM head, in order to minimize oxygen loss from the sample surfaces. Mechanically sharpened Pt-Ir alloys were used as STM tips.

Figure 1(a) shows a set of empty-state STM images obtained on the cleaved *ab* surfaces of Pb-Bi2212 single crystals for different bias voltages at 4.3 K. As previously reported, the Pb-Bi2212 crystals used in this study show lamella-type phase separation into a modulated α phase and a modulation-free β phase.[6,9–12] The STM images in Fig. 1(a) were taken on the α phase region with a modulation structure along the *b* axis with a periodicity of ~6 nm, which is highly elongated compared to pure Bi2212 due to the Bi/Pb substitution.[6,9–12] In the images obtained using lower bias voltages, a square lattice network of Bi atoms is visible together with several brighter atoms. As described in

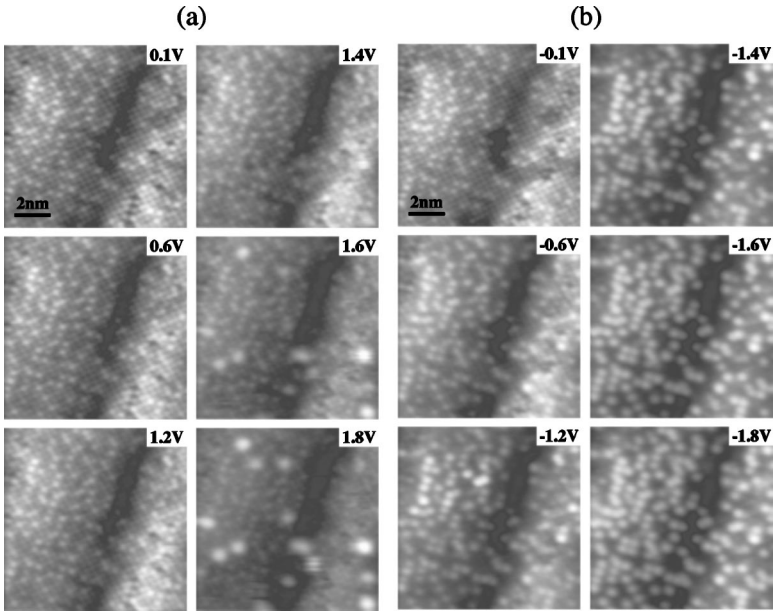

FIG. 1. STM images of Pb-Bi2212 taken at (a) positive and (b) negative bias voltages as indicated in the each image at 4.3 K. The tunneling current was fixed at 0.4 nA.

the previous report,[6] these are identified as Pb atoms substituted into Bi sites. At higher bias conditions, $V_{sample}(V_s) > 1.4$ V, in contrast, new brighter spots suddenly appear. Their corrugations are enhanced as V_s is increased further, while the contrast of Pb atoms is essentially unchanged in the empty-state images.

Figure 1(b) shows filled-state STM images obtained with negative bias voltages, with the imaged region selected to be identical to that shown in Fig. 1(a). At $V_s = -0.1$ V, the square lattice pattern consisting of Bi and Pb atoms is nearly identical to the pattern at positive bias. Interestingly, however, the contrast of the Pb atoms is significantly increased at higher $|V_s|$. We have checked and verified that the bias-dependent STM images described above are reproducible, even after cycling V_s, between +2.0 and −2.0 V.

Figure 2 shows narrow-scan STM images taken at three different values of V_s. When V_s is set to +1.8 V, an atomic structure with a large corrugation, marked by an open circle, appears at the center of the image [Fig. 2(b)]. On the other hand, this structure is completely missing in the images observed with small or negative V_s, as shown in Figs. 2(a) and 2(c), for a V_s value of 0.1 and −1.8 V, respectively. By comparing Figs. 2(a) and 2(b), it is evident that the atomic structure emerging at $V_s = +1.8$ V is located at the center of a square connecting four Bi(Pb) atoms. Considering the crystal structure of Bi2212, we tentatively conclude that this structure originates from impurities or defects occupying the Sr or Ca site, which is located approximately 0.3 or 0.6 nm, respectively, beneath the top BiO layer. The population of Sr(Ca) site impurities is estimated to be ~3%, which is much lower than that of Pb atoms replacing the Bi sites, which is 20%-24%.[6]

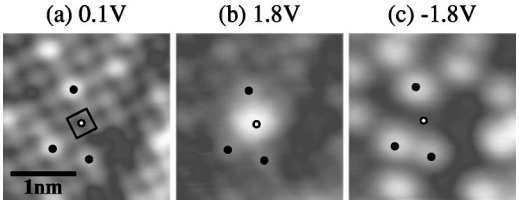

FIG. 2. Narrow-scan STM images of Pb-Bi2212 at 4.3 K. The tunneling conditions were (a) $V_s = 0.1$ V and $I_t = 0.5$ nA, (b) $V_s = 1.8$ V and $I_t = 1.0$ nA, and (c) $V_s = -1.8$ V and $I_t = 0.6$ nA.

In order to determine how the two types of impurities modify the electronic structure of Bi2212, we performed STM/STS measurements over an energy range of ±2 V at 4.3 K. Figure 3(a) shows an STM image taken at 1.8 V and conductance maps at various V_s values ranging from +0.4 to +1.8 *V*, which correspond to spatial distributions of local density of states at $E = eV_s$, $N(eV)$. As can be seen, the conductance maps at $V_s < 1.2$ V reveal an almost homogeneous LDOS. As V_s is increased from 1.2 V, however, round structures with elevated LDOS begin to evolve, and their locations are in good agreement with those of the bright spots in the STM image.

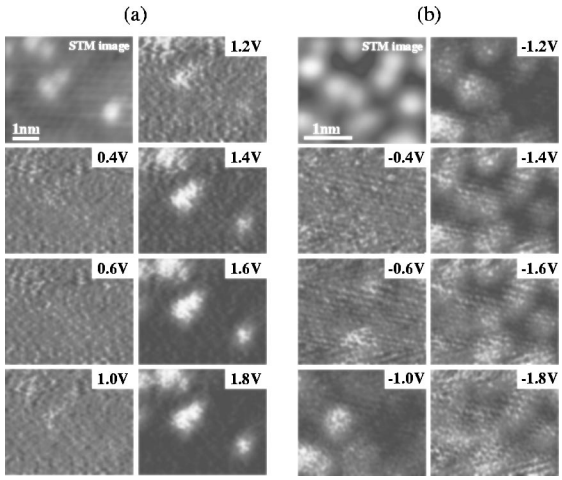

FIG. 3. Differential conductance images of Pb-Bi2212 at (a) positive and (b) negative bias voltages at 4.3 K. The differential conductance values were normalized at (a) +0.2 V and (b) −0.2 V. Tunneling conditions were (a) $V_s = 1.8$ V and $I_t = 0.4$ nA, and (b) $V_s = -1.8$ V and $I_t = 0.6$ nA.

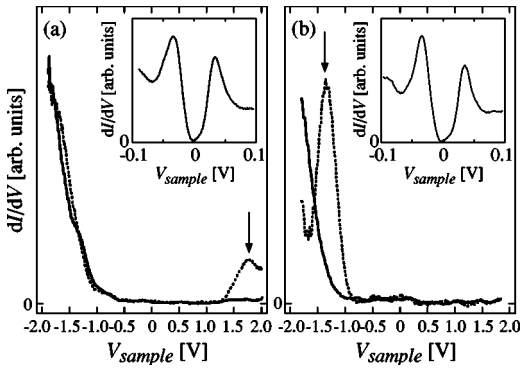

FIG. 4. Tunneling spectra obtained for various impurity sites imaged as shown in Fig. 3. (a) Tunneling spectra taken for an Sr(Ca)-site impurity (dotted line). (b) Tunneling spectra taken for a Pb atom (dotted line). The solid lines are "normal" spectra taken at locations far away from impurity sites. These spectra are normalized to (a) 0.2 V and(b) −0.2 V. The insets in (a) and (b) show high-resolution spectra around the Fermi level, obtained for the Sr(Ca)-site impurity and the Pb atom, respectively.

Figure 3(b) shows another STM/STS result taken at 4.3 K for negative bias voltages. The STM image recorded with $V_s = -1.8$ V clearly resolves several Pb atoms. Again, the corresponding conductance map at $V_s > -0.6$ V is rather uniform and does not show any specific structure around Pb atoms. However, it was found that LDOS around the Pb atoms is significantly enhanced when the bias voltage was lower than −0.6 V.

Figure 4(a) compares a typical tunneling spectrum obtained for a Sr(Ca)-site impurity (dotted line) with a "normal" spectrum obtained at a location far from the impurity site (solid line). The former clearly shows a localized impurity state around +1.7 eV above the Fermi level, as indicated by the arrow, which is thought to behave as a deep donor below the conduction band, similar to *n*-type-doped semiconductors. This strongly suggests that the impurity ions substituting for Sr^{2+} or Ca^{2+} sites possess a valence higher than +2. It is well known that Sr sites in Bi2212 are often replaced by excess Bi^{3+} ions, as expressed by the chemical formula $Bi_{2+x}Sr_{2-x}CaCu_2O_y$, because the additional positive charges introduced by the Bi^{3+}/Sr^{2+} substitution substantially stabilize the crystal structure.[15–17] The excess Bi amount x is typically ~ 0.1,[17] which is in good agreement with the population of Sr(Ca)-site impurities, ~3%, estimated from the STM images in this study. Therefore, we speculate that the impurity states around +1.7 eV are caused by Bi^{3+} ions substituting for Sr^{2+} sites.

Next, we consider the tunneling conductance near zero bias. In Fig. 4(a), no superconducting energy gap can be resolved because of insufficient energy resolution. The inset in Fig. 4(a) shows the superconducting density of states obtained for the impurity site with better energy resolution $\Delta E \sim 1$ meV. A superconducting gap structure with $2\Delta \sim 70$ meV is clearly seen from the figure, but there is no conductance peak arising from quasiparticle scattering near the Fermi level, contrary to the STM/STS observations of Zn- (Ref. 13) and Ni-doped Bi2212 single crystals.[14] In Fig. 4, we set the energy resolution to 1 meV, which is sufficiently high to detect quasiparticle resonant peaks, as previously reported.[18] This proves that the Sr(Ca)-site impurity does not act as a pair breaker.

Figure 4(b) shows the tunneling spectrum taken for a Pb atom. Again, the higher energy resolution spectrum at the Pb site reveals a well-developed superconducting gap, as shown in the inset. It is to be noted that the spectrum at the Pb site (dotted line) shows an acceptorlike level at −1.4 eV, although it almost overlaps with the valence-band edge. This can be qualitatively understood by assuming that covalent Pb^{2+} ions are substituted for trivalent Bi^{3+} ions. We evaluated the Bohr radius r_0 of electron (hole) orbits around donors (acceptors) by fitting an $\exp(-r/r_0)$ function to the conductance images around the isolated impurities. The resultant r_0 values are approximately 0.3 nm for both the Sr site impurities and Pb atoms, which is about one order of magnitude smaller than the r_0 values in conventional semiconductors such as Si and Ge. This indicates that the impurity states observed in this study are extremely localized due to a relatively small dielectric constant or a large electron mass.

In summary, we determined the local electronic properties of substitutional impurities located in the blocking layers in high-T_c cuprate Bi2212 single crystals, using low-temperature STM/STS measurements. The Sr(Ca)-site impurities were found to form localized donor states at 1.7 eV above the Fermi level, while acceptorlike states appeared at −1.4 eV near the valence-band edge as a consequence of Bi/Pb replacement. These suggest to us the chemical view wherein Bi^{2+}, substitutes for Sr^{2+}, and Pb^{2+} for Bi^{3+}. In addition, both states showed little influence on the LDOS near the Fermi level, indicating that they do not behave as pinning centers.

*Electronic address: kinoda@ksp.or.jp

†Also at Kanagawa Academy of Science and Technology.

[1] R. de Kort, M. C. M. M. van der Wielen, A. J. A. van Roij, W. Kets, and H. van Kempen, Phys. Rev. B **63**, 125336 (2001).

[2] J. Gebauer, E. R. Weber, N. D. Jäger, K. Urban, and Ph. Ebert, Appl. Phys. Lett. **82**, 2059 (2003).

[3] A. M. Yakunin, A. Yu. Silov, P. M. Koenraad, J. H. Wolter, W. Van Roy, J. De Boeck, J.-M. Tang, and M. E. Flatté, Phys. Rev. Lett. **92**, 216806 (2004).

[4] M. Schöck, C. Sürgers, and H. v. Löhneysen, Phys. Rev. B **61**, 7622 (2000).

[5] C. Sürgers, M. Schöck, T. Trappmann, and H. v. Löhneysen, Appl. Surf. Sci. **212-213**, 105 (2003).

[6] G. Kinoda, T. Hasegawa, S. Nakao, T. Hanaguri, K. Kitazawa, K. Shimizu, J. Shimoyama, and K. Kishio, Phys. Rev. B **67**, 224509 (2003).

[7] T. Motohashi, Y. Nakayama, T. Fujita, K. Kitazawa, J. Shimoyama, and K. Kishio, Phys. Rev. B **59**, 14080 (1999).

[8] G. Kinoda, T. Yamanouchi, H. Suzuki, T. Endo, K. Kitazawa, and T. Hasegawa, Physica C **353**, 297 (2001).
[9] I. Chong, Z. Hiroi, J. Shimoyama, Y. Nakayama, K. Kishio, T. Terashima, Y. Bando, and M. Takano, Science **276**, 770 (1997).
[10] S. Nakao, K. Ueno, T. Hanaguri, K. Kitazawa, T. Fujita, Y. Nakayama, T. Motohashi, J. Shimoyama, K. Kishio, and T. Hasegawa, J. Low Temp. Phys. **117**, 341 (1999).
[11] M. Nishiyama, K. Ogawa, I. Chong, Z. Hiroi, and M. Takano, Physica C **314**, 229 (1999).
[12] G. Kinoda, T. Hasegawa, S. Nakao, T. Hanaguri, K. Kitazawa, K. Shimizu, J. Shimoyama, and K. Kishio, Appl. Phys. Lett. **83**, 1178 (2003).
[13] S. H. Pan, E. W. Hudson, K. M. Lang, H. Eisaki, S. Uchida, and J. C. Davis, Nature (London) **403**, 746 (2000).
[14] W. E. Hudson, K. M. Lang, V. Madhavan, S. H. Pan, H. Eisaki, S. Uchida, and J. C. Davis, Nature (London) **411**, 920 (2001).
[15] Y. Ikeda, H. Ito, S. Shimomura, Y. Oue, K. Inaba, Z. Hiroi, and M. Takano, Physica C **159**, 93 (1989).
[16] H. E. Zandbergen, W. A. Groen, A. Smit, and G. Vantendeloo, Physica C **168**, 426 (1990).
[17] H. Eisaki, N. Kaneko, D. L. Feng, A. Damascelli, P. K. Mang, K. M. Shen, Z.-X. Shen, and M. Greven, Phys. Rev. B **69**, 064512 (2004).
[18] G. Kinoda, H. Mashima, S. Nakao, K. Shimizu, J. Shimoyama, K. Kishio, T. Hanaguri, K. Kitazawa, and T. Hasegawa, AIP Conf. Proc. **696**, 888 (2003).